2006

Carbohydrate doping to enhance electromagnetic properties of MgB2 superconductors

Jung Ho Kim
University of Wollongong, jhk@uow.edu.au

Sihai Zhou
University of Wollongong, sihai@uow.edu.au

Md S. Hossain
University of Wollongong, shahriar@uow.edu.au

Alexey V. Pan
University of Wollongong, pan@uow.edu.au

S X. Dou
University of Wollongong, shi@uow.edu.au

Publication Details

Kim, J, Zhou, S, Hossain, M, Pan, AV & Dou, SX (2006), Carbohydrate doping to enhance electromagnetic properties of MgB2 superconductors, Applied Physics Letters, 89(14), pp. 142505-1-142505-3.

Carbohydrate doping to enhance electromagnetic properties of MgB2 superconductors

Abstract
The effect of carbohydrate doping on lattice parameters, microstructure, T_c, J_c, H_{irr}, and H_{c2} of MgB_2 has been studied. In this work the authors used malic acid as an example of carbohydrates as an additive to MgB_2. The advantages of carbohydrate doping include homogeneous mixing of precursor powders, avoidance of expansive nanoadditives, production of highly reactive C, and significant enhancement in J_c, H_{irr}, and Hc_2 of MgB_2, compared to undoped samples. The J_c for MgB_2+30 wt% $C_4H_6O_5$ sample was increased by a factor of 21 at 5 K and 8 T without degradation of self-field J_c.

Keywords
Carbohydrate, doping, enhance, electromagnetic, properties, MgB2, superconductors

Disciplines
Engineering | Physical Sciences and Mathematics

Publication Details
Kim, J, Zhou, S, Hossain, M, Pan, AV & Dou, SX (2006), Carbohydrate doping to enhance electromagnetic properties of MgB2 superconductors, Applied Physics Letters, 89(14), pp. 142505-1-142505-3.

Carbohydrate doping to enhance electromagnetic properties of MgB_2 superconductors

J. H. Kim, S. Zhou, M. S. A. Hossain, A. V. Pan, and S. X. Dou[a)]
Institute for Superconducting and Electronic Materials, University of Wollongong, Northfields Ave., Wollongong, New South Wales 2522, Australia

(Received 21 July 2006; accepted 23 August 2006; published online 3 October 2006)

The effect of carbohydrate doping on lattice parameters, microstructure, T_c, J_c, H_{irr}, and H_{c2} of MgB_2 has been studied. In this work the authors used malic acid as an example of carbohydrates as an additive to MgB_2. The advantages of carbohydrate doping include homogeneous mixing of precursor powders, avoidance of expansive nanoadditives, production of highly reactive C, and significant enhancement in J_c, H_{irr}, and H_{c2} of MgB_2, compared to undoped samples. The J_c for MgB_2+30 wt % $C_4H_6O_5$ sample was increased by a factor of 21 at 5 K and 8 T without degradation of self-field J_c. © *2006 American Institute of Physics*. [DOI: 10.1063/1.2358947]

With the relatively high critical temperature (T_c) of 39 K (Ref. 1) and the high critical current density (J_c) of $>10^5$ cm^{-2} in moderate fields, magnesium diboride (MgB_2) superconductors could offer the promise of important large-scale applications to be operated at 20 K. A significant enhancement in the electromagnetic properties of MgB_2 has been achieved through doping with various forms of carbon (C).[2–6] To take advantage of its T_c of 39 K, enhancements of both the upper critical field (H_{c2}) and J_c are essential. Attempts to accomplish this have invoked the introduction of numerous techniques including chemical doping,[2–6] irradiation,[7] and various thermomechanical processing techniques.[8,9] Chemical doping is a simple and readily scalable technique. Since MgB_2 has a relatively large coherence length and small anisotropy, the fluxoids to be pinned are stringlike and amenable to pinning by inclusions and precipitates in the grains.

Among the numerous forms of C-containing dopants, SiC doping has achieved a record high in-field $J_c(B)$, H_{c2}, and irreversibility (H_{irr}) in MgB_2.[2] These record high properties have been confirmed and reproduced by many groups,[2,5,10,11] and the performance records remain unbroken up to now. However, the best high-field J_c values achieved in the SiC doped MgB_2 wires were compromised by the reduction in self-field and low-field J_c. Although nanosize precursor particles were chosen for the doping process it is a great challenge to achieve homogeneous distribution of a small amount of nanodopants within the matrix materials through solid state mixing. There are always agglomerates of nanoadditives in the precursors. For various forms of C doping, the substitution of C for boron (B) cannot be achieved at the same temperatures as that of the MgB_2 formation reaction due to their poor reactivity.

In order to overcome these problems we proposed to use a carbohydrate such as DL-malic acid ($C_4H_6O_5$) as the dopant. The significant advantages of carbohydrate are as follows. (1) Carbohydrates can be dissolved in a solvent so that the solution can form a slurry with B powder. After evaporating the solvent the carbohydrate forms a coating on the B powder surfaces, giving a highly uniform mixture. (2) The carbohydrates in the mixture melt at lower temperatures and decompose at temperatures below the formation temperature of MgB_2, hence producing highly reactive and fresh C on the atomic scale, as well as a reducing reagent, carbon monoxide, which may convert boron oxide to B, reducing the impurities in B powder. (3) Because of the high reactivity of the freshly formed C, the C substitution for B can take place at the same temperature as the formation temperature of MgB_2. The simultaneous dual reactions promote C substitution for B in the lattice and the inclusion of excess C within the grains, resulting in the enhancement of J_c, H_{irr}, and H_{c2}.

In this study, therefore, we used malic acid as a representative of carbohydrate dopant. We fabricated MgB_2 +$C_4H_6O_5$ samples with different addition levels. The lattice parameters T_c, J_c, H_{irr}, H_{c2}, and microstructures are presented in comparison with the undoped reference MgB_2. MgB_2 pellets were prepared by an *in situ* reaction process with the addition of $C_4H_6O_5$. The selected amount of $C_4H_6O_5$ (99%), from 0 to 30 wt % of total MgB_2 was mixed with an appropriate amount of B (99%) powder in toluene (C_7H_8, 99.5%). This slurry was dried in vacuum so that the B powder particles were coated by the C coming from $C_4H_6O_5$. Since the decomposition temperature of $C_4H_6O_5$ was at around 150 °C, this uniform composite was then mixed with an appropriate amount of Mg (99%) powder. These mixed powders were ground, pressed, and then sintered at 900 °C for 30 min under argon gas. All samples were characterized by x-ray diffraction (XRD), field emission gun-scanning electron microscopy (FEG-SEM), J_c, T_c, H_{irr}, and H_{c2}.[3] The lattice parameters were obtained from Rietveld refinement.

Table I shows the measured data for the undoped MgB_2 and MgB_2+$C_4H_6O_5$ samples with different addition levels. The lattice parameters calculated from XRD show a large decrease in the *a*-axis parameter with 10 wt % $C_4H_6O_5$ and a small further drop in *a* with increasing $C_4H_6O_5$ addition level, but no change in the *c*-axis parameter. This is an indication of the C substitution for B. The actual C substitution level can be estimated from the *a*-axis change.[12] It should be noted that the net C percentage addition is only 36% of the $C_4H_6O_5$ addition. The actual C substitution levels of 1.9–2.3 at % of B at three doping levels are clearly higher than those with other forms of C dopants, which is attributable to the high reactivity of fresh C released from the de-

[a)]Author to whom correspondence should be addressed; electronic mail: shi_dou@uow.edu.au

TABLE I. Measured data for undoped MgB_2 and $MgB_2+C_4H_6O_5$ samples with different addition levels. H^*_{irr} was calculated from the standard criterion of J_c (100 A cm^{-2}).

Malic acid ($C_4H_6O_5$) amount (wt %)	Lattice parameters a (Å)	Lattice parameters c (Å)	Actual C (x) in $MgB_{2-x}C_x$ [a]	T_c (K)	$\rho_{40\ K}$ ($\mu\Omega$ cm)	$\rho_{300\ K}$ ($\mu\Omega$ cm)	H^*_{irr} (T) (20 K)	J_c (A cm^{-2}) Self-field (20 K)	J_c (A cm^{-2}) 8 T (5 K)
0	3.0835(5)	3.5217(5)		37.6	34.5	73.5	5.4	3.9×10^5	0.1×10^4
10	3.0751(6)	3.5268(3)	0.0380	35.8	90.2	146.5	6.7	3.5×10^5	2.3×10^4
20	3.0746(4)	3.5229(7)	0.0404	35.7	83.8	146.2	6.8	3.5×10^5	2.7×10^4
30	3.0731(9)	3.5214(7)	0.0460	35.8	79.6	131.9	6.7	4.0×10^5	2.6×10^4

[a]Extrapolation from measured lattice parameters (Ref. 12).

composition of $C_4H_6O_5$ at low temperature. The increase in sintering temperature improves both the crystallinity and the C substitution for B. The former will increase T_c, while the latter will decrease T_c. As a compromise, these two opposing factors result in a high level of C substitution for B with a relatively small drop in T_c. The high-field J_c's of the $MgB_2+C_4H_6O_5$ samples were much higher than that of the undoped MgB_2. Specifically, it should be noted that the self-field J_c of $MgB_2+C_4H_6O_5$ samples was not reduced at addition levels as high as 30 wt % $C_4H_6O_5$; hence the connectivity between MgB_2 grains was not affected by addition with $C_4H_6O_5$. Although there is a possibility of the formation of H_2O during sintering due to the decomposition of $C_4H_6O_5$, there was no degradation in self-field J_c, even for 30 wt % $C_4H_6O_5$ added to MgB_2. This may be attributable to the fact that the decomposition products, C and CO, of $C_4H_6O_5$ reduced B_2O_3 and hence increased the effective cross section of the superconductor.

Figure 1(a) shows the magnetic field dependence of J_c in all samples at 20 and 5 K. It should be noted that J_c values in high field were increased by more than an order of magnitude. For example, the J_c value of 2.5×10^4 A cm^{-2} at 5 K and 8 T for MgB_2+30 wt % $C_4H_6O_5$ sample is higher than that of the undoped MgB_2 by a factor of 21. In addition, there was no J_c degradation in self-field for the MgB_2+30 wt % $C_4H_6O_5$ sample. These findings can be further supported by the flux pinning results. Figure 1(b) plots the field dependence of the volume pinning force, $F_p=J\times B$, of all samples at 20 K. The F_p is normalized by the maximum volume pinning force $F_{p,\max}$. The flux pinning for the $MgB_2+C_4H_6O_5$ samples was significantly higher than that of the undoped one at $B>1.5$ T. This result indicates that the $F_p(B)$ of $MgB_2+C_4H_6O_5$ samples was improved by the C substitution effect and nano-C inclusions within the grains.

The normalized temperature dependence of H_{irr} and H_{c2} for all samples is shown in Fig. 2. Significantly enhanced H_{irr} and H_{c2} for $MgB_2+C_4H_6O_5$ samples were observed, suggesting that C substitution into B sites results in an enhancement in H_{irr} and H_{c2}. The steeper slopes of H_{irr} for $MgB_2+C_4H_6O_5$ samples exceeded H_{c2} of undoped MgB_2 below a

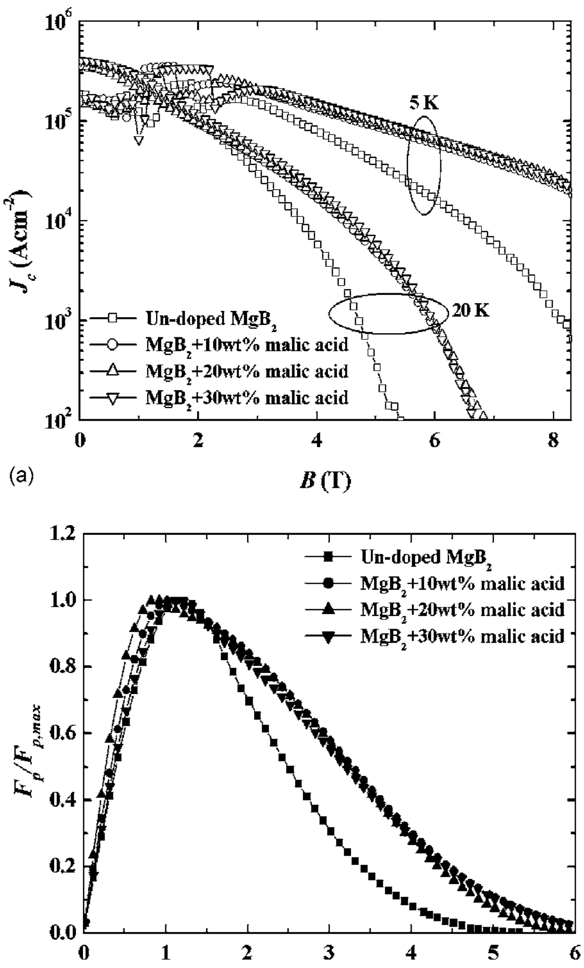

FIG. 1. Superconducting properties of undoped MgB_2 and $MgB_2+C_4H_6O_5$ samples with different addition levels: (a) Magnetic field dependence of J_c in all samples at 20 and 5 K; (b) field dependence of the volume pinning force, $F_p=J\times B$, of all samples at 20 K. The F_p is normalized by the maximum volume pinning force $F_{p,\max}$.

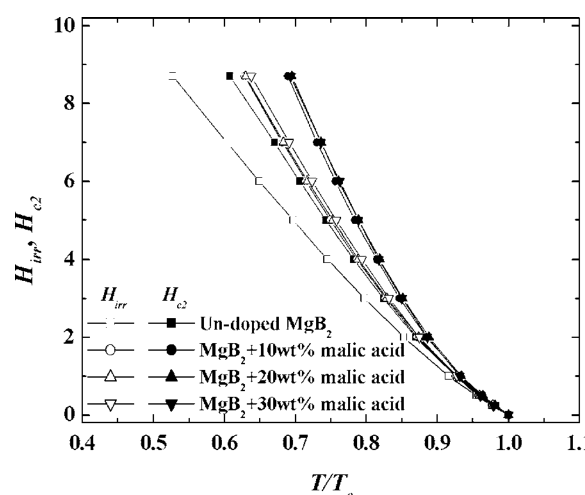

FIG. 2. Normalized temperature dependence of H_{irr} and H_{c2} for undoped and $C_4H_6O_5$ doped samples. H_{c2} and H_{irr} were defined as $H_{c2}=0.9R(T_c)$ and $H_{irr}=0.1R(T_c)$ from the R vs T curve.

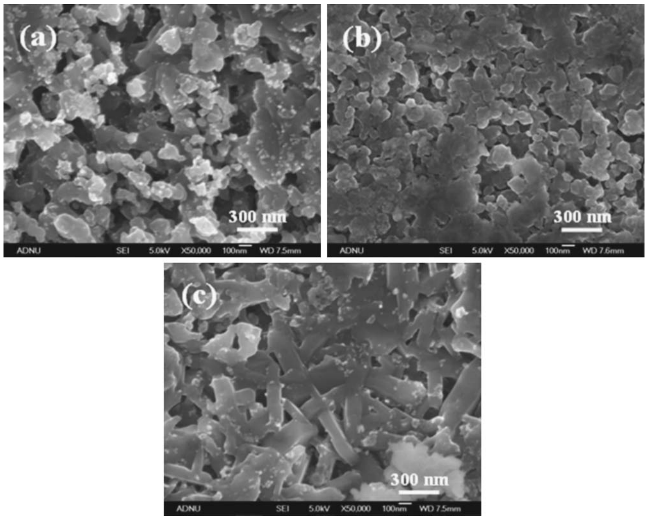

FIG. 3. Photographs from FEG-SEM: (a) Undoped MgB_2, (b) MgB_2 +10 wt % $C_4H_6O_5$, and (c) MgB_2+30 wt % $C_4H_6O_5$.

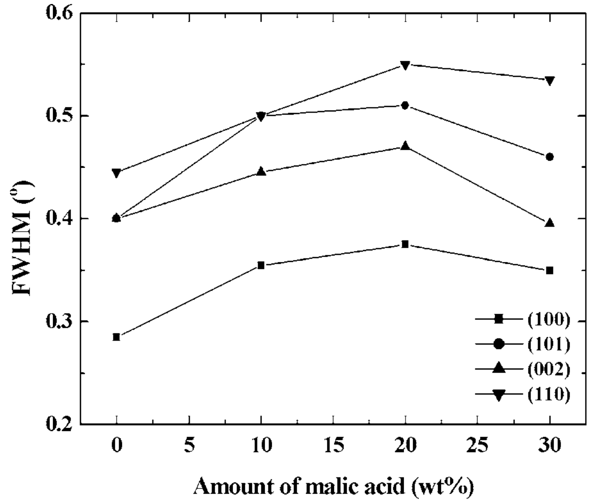

FIG. 4. FWHM as a function of the amount of $C_4H_6O_5$. MgB_2(100), (101), (002), and (110) correspond to $2\theta \sim 33.6°$, 42.5°, 52.0°, and 60.0°, respectively.

temperature of 22 K. The resistivities ρ for the undoped and $MgB_2+C_4H_6O_5$ samples are 34 and 80–90 $\mu\Omega$ cm at 40 K, respectively, as shown in Table I. The increased resistivity for $MgB_2+C_4H_6O_5$ samples indicates the increased impurity scattering as a result of C substitution into B sites.

FEG-SEM images for (a) undoped MgB_2, (b) MgB_2 +10 wt % $C_4H_6O_5$, and (c) MgB_2+30 wt % $C_4H_6O_5$ are shown in Fig. 3. The undoped MgB_2 sample appears inhomogeneous, consisting of crystalline grains from several tens of nanometers in size to 500 nm. The morphology of the MgB_2+10 wt % $C_4H_6O_5$ sample was refined to smaller, denser, and more homogeneous grains compared to the undoped MgB_2 one. The grain refinement by 10 and 20 wt % $C_4H_6O_5$ additions is supported by the full width at half maximum (FWHM) results for all the peaks, as shown in Fig. 4. As the doping level further increases to 30 wt %, however, grains appear to have a bar/plate shape, with their width up to 150 nm and length up to 400 nm, in a well connected grain network [Fig. 3(c)]. Consistent with the FEG-SEM image is the decrease in FWHM for the 30 wt % doped sample (Fig. 4) although the average FWHM values for all peaks are still bigger than those of the undoped sample. The FEG-SEM image suggests that at higher addition levels $C_4H_6O_5$ may act as a sintering aid to improve the crystallinity. The grain growth should not improve the electromagnetic properties. However, this effect may be offset by the increase in C substitution level, the reduction in resistivity (Table I), and improvement in grain connectivity. This is well evidenced by the fact that the self-field J_c of the MgB_2+30 wt % $C_4H_6O_5$ sample was enhanced while the improved in-field J_c, H_{irr}, and H_{c2} were maintained, as shown in Figs. 1 and 2.

In summary, carbohydrate doping results in a small depression in T_c but significantly increases the C substitution level, reduces the impurities, and hence improves J_c, H_{irr}, and H_{c2} performances at all the operating temperatures and over the entire field range. This finding opens a direction for the manufacture of nanodoped materials using the carbohydrate solution route, which solves the agglomeration problem, avoids the use of expensive nanoadditives, and achieves improved performance properties.

The authors gratefully acknowledge helpful discussion with E. W. Collings and M. Tomsic, and financial support from the Australian Research Council, Hyper Tech Research Inc., and CMS Alphatech International Ltd.

[1]J. Nagamatsu, N. Nakagawa, T. Muranaka, Y. Zenitani, and J. Akimitsu, Nature (London) **410**, 63 (2001).
[2]S. X. Dou, S. Soltanian, J. Horvat, X. L. Wang, S. H. Zhou, M. Ionescu, H. K. Liu, P. Munroe, and M. Tomsic, Appl. Phys. Lett. **81**, 3419 (2002).
[3]J. H. Kim, W. K. Yeoh, M. J. Qin, X. Xu, and S. X. Dou, J. Appl. Phys. **100**, 013908 (2006).
[4]R. H. T. Wilke, S. L. Bud'ko, P. C. Canfield, D. K. Finnemore, R. J. Suplinskas, and S. T. Hannahs, Phys. Rev. Lett. **92**, 217003 (2004).
[5]H. Kumakura, H. Kitaguchi, A. Matsumoto, and H. Hatakeyama, Appl. Phys. Lett. **84**, 3669 (2004).
[6]A. Yamamoto, J. I. Shimoyama, S. Ueda, I. Iwayama, S. Horii, and K. Kishio, Supercond. Sci. Technol. **18**, 1323 (2005).
[7]Y. Bugoslavsky, G. K. Perkins, X. Qi, L. F. Cohen, and A. D. Caplin, Nature (London) **410**, 561 (2001).
[8]R. Flükiger, H. L. Suo, N. Musolino, C. Beneduce, P. Toulemonde, and P. Lezza, Physica C **385**, 286 (2003).
[9]A. Serquis, L. Civale, D. L. Hammon, X. Z. Liao, J. Y. Coulter, Y. T. Zhu, M. Jaime, D. E. Peterson, and F. M. Mueller, Appl. Phys. Lett. **82**, 2847 (2002).
[10]H. Yamada, M. Hirakawa, H. Kumakura, and H. Kitaguchi, Supercond. Sci. Technol. **19**, 175 (2006).
[11]M. D. Sumption, M. Bhatia, M. Rindfleisch, M. Tomsic, S. Soltanian, S. X. Dou, and E. W. Collings, Appl. Phys. Lett. **86**, 092507 (2005).
[12]S. Lee, T. Masui, A. Yamamoto, H. Uchitama, and S. Takama, Physica C **397**, 7 (2003).